

Three-Dimensional Direct Simulation Monte Carlo Method for Slider Air Bearings

Weidong Huang and David B. Bogy

Computer Mechanics Laboratory
Department of Mechanical Engineering
University of California
Berkeley, CA 94720

Alejandro L. Garcia

Department of Physics
San Jose State University
San Jose, CA 95192

Abstract

The direct simulation Monte Carlo (DSMC) method is used to solve the three-dimensional nano-scale gas film lubrication problem between a gas bearing slider and a rotating disk, and this solution is compared to the numerical solution of the compressible Reynolds equations with the slip flow correction based on the linearized Boltzmann equation as presented by Fukui and Kaneko (MGL method¹). In the DSMC method, hundreds of thousands of simulated particles are used and their three velocity components and three spatial coordinates are calculated and recorded by using a hard-sphere collision model. Two-dimensional pressure profiles are obtained across the film thickness direction. The results obtained from the two methods agree well with each other for Knudsen numbers as large as 35 which corresponds to a minimum spacing of 2 nm. The result for contact slider is also obtained by the DSMC simulation and presented in this paper.

I. Introduction

Slider air bearing modeling requires increased accuracy for lower spacings in today's hard-disk industry. In order to increase the magnetic recording density, the read/write head is required to fly lower, now approaching contact with the hard disk surface. On the other hand tribological considerations dictate the continued reliance on air bearings to support most of the interface load. In current drives, the slider carrying the read/write head flies within the range of the mean free path of the gas molecules λ , ($\lambda = 65$ nm at STP for air). The air bearing force and flying height prediction is crucial in slider air bearing design.

In the head/disk interface, the rotation of the disk surface brings air under the slider that creates the pressure and provides the lifting force that causes the head to float above the disk. Traditionally, macroscopic hydrodynamic equations (e.g. Navier-Stokes. Reynolds) have been used to model slider air bearing problems. In 1867, Maxwell discovered the “velocity slip” effect near a moving wall. The slip correction was introduced into the Reynolds equation by Burgdorfer in 1959 for Knudsen numbers $Kn \ll 1$, where Kn is defined as the ratio of the molecular mean free path to the characteristic length of the flow. Hsia (1983) proposed a higher order approximation for larger Knudsen numbers. Fukui and Kaneko (1988) developed a more sophisticated slip correction for the Reynolds equation, based on the Boltzmann equation, where the Poiseuille flow rate was calculated on the basis of a linearized BGK¹ model of the Boltzmann equation. The validity of this model (often referred as the MGL model) was confirmed in the range of a Kn up to 6, that is, for minimum spacing of 10 nm under standard atmospheric pressure (Takeuchi et al., 1994). In the Computer Mechanics Laboratory (CML) at Berkeley, the CML Air Bearing Design Program has been developed (Lu and Bogy, 1995). This program uses

the compressible Reynolds equation with various slip corrections for rarefied flows, which was solved by a multi-grid control volume method for the simulation of arbitrarily shaped slider air bearings with multiple recess levels.

The Direct Simulation Monte Carlo (DSMC) approach was first employed for the slider air bearing problem by Alexander et al. (1994). They considered a 5 μm long flat slider of infinite width. Their results showed that for such a two-dimensional flat slider, the MGL model gives accurate results, even in regimes where its validity should be questionable.

The MGL model needs further verification for slider air bearing designs under several circumstances: (i) When the slider geometry is 3-dimensional, i.e. side effects are taken into account, (ii) When the flow is 3-dimensional due to either slider configuration or surface roughness, (iii) when the application of interest is close to quasi-contact or contact.

The Direct Simulation Monte Carlo method has been thoroughly tested over the past 20 years and found to be in excellent agreement with both molecular dynamics and experiments. It is loosely based on the Boltzmann equation and was popularized as a practical numerical algorithm by G. A. Bird in the late 60's. In the slider air bearing problem, the DSMC method can be applied to various surface configurations, such as those with surface roughness. The flow is no longer assumed to be a plane flow, as required by lubrication theory.

The objectives of this project are: (i) the determination of the validity of the 3-dimensional slider bearing models for minimum spacings below 25 nm, (ii) the investigation of the model for quasi-contact and contact. In this report, we present the results from DSMC simulations of the 3-dimensional flat slider bearing problem.

Following this introduction, Part II describes the DSMC algorithm and numerical system configuration for the slider bearing problem. Part III presents the DSMC simulation results and

compares them to the MGL model. Then a summary and comments on future work are given in Part IV.

II. DSMC Method

Instead of using molecular dynamics to keep track of a huge number of molecules, DSMC, which was constructed as a stochastic model, abandons the attempt to predict the instantaneous state of a simulated particle and only provides probabilities and average quantities. Even in a very small volume, we are still averaging over a large sample. For example, at STP, there will be about 6,200 air molecules in a volume of a cubic mean free path. Each particle used by DSMC represents a number of real molecules that are roughly at the same position with roughly the same velocity.

The gas under the slider is assumed to be dilute so that the interactions between particles are modeled as two-body collisions and the potential energy of the particles is negligible compared to the kinetic energy. We use a hard sphere model throughout this report. The particles behave like a cloud of tiny billiard balls of diameter d . The simulation region is divided into rectangular cells. For reliable simulations, the DSMC method requires that the cell volumes are no larger than a cubic mean-free-path, and in each cell there should be an average of at least 20 ~ 30 simulated particles (Alexander et al. 1994).

In the simulation, the state of the system is given by the positions and velocities of particles, $\{ \mathbf{r}_i, \mathbf{v}_i \}$. At each time step, particles are moved with free flight motion. Any particles that reach a boundary are processed according to the appropriate boundary condition. After all particles finish moving for one time step, some particles are selected randomly for collisions (Garcia, 1994). The number of collision candidates per cell within one time step is determined by:

$$M_{candidate} = \frac{N_{cell}^2 \pi d^2 v_r^{max} \tau}{2V_{cell}} \quad (1)$$

where N_{cell} = Number of particles in a cell

d = Diameter of the particle

v_r^{max} = Estimated maximum relative speed between particles (three times the most probable particle velocity)

τ = time step

V_{cell} = Effective cell volume

Only those particles in the same cell can be selected as collision partners, regardless of their positions within the cell. The selection is random. After the collision candidates are determined, the probability of whether they are accepted or rejected for collision is calculated based on their relative speed according to the hard sphere model. In our simulations, about 1% ~ 2% of the total particles are selected to collide with other particles within every time step. Once the collision pairs are chosen, their post-collision velocities are evaluated by the conservation of linear momentum and energy. The velocities and positions of particles are recorded for later averaging.

The DSMC method is based on the assumption that when the time step is less than the mean collision time for a particle, which is defined as the mean time between the successive collisions of any particle, the particle collisions can be decoupled from the particle positional changes within one time step. The time step we used is one fifth of the time a particle needs to pass through a single cell with the most probable velocity (337 m/s for the argon atom at STP).

There are two types of boundary conditions in our simulation for the slider bearing problem: thermal walls and fluxing reservoirs. The slider and disk surfaces are two thermal walls. When a particle strikes either of these walls, the particle velocity is reset according to a

biased Maxwellian distribution. The four sides of the slider are treated as fluxing reservoirs. They act as infinite, equilibrium thermal baths at temperature T_0 and pressure P_0 . The flow velocity in the reservoirs are such that the pressure at all four sides can be maintained at ambient pressure P_0 . Due to the fact that the particles are traveling at much higher speed than the disk, it is very easy for particles to enter the control volume from the exit.

To get the averaged quantities, such as momentum and kinetic energy, the program does the sampling after the flow system reaches its steady state. We use the total number of particles inside the system to be the indicator of the steady state. The program starts sampling when the total particle number becomes steady.

III. DSMC Simulation and Results

Figure 1 shows a typical 3-D flat slider gas bearing configuration. The length L of the slider is $4\ \mu\text{m}$, its width W is $3.3\ \mu\text{m}$. The height at the trailing edge of the slider, H_{\min} , which is used to determine the Knudsen number, ranges from $25\ \text{nm}$ to $0\ \text{nm}$. The pitch angle α is 0.01 rad. The disk speed U at the slider is $25\ \text{m/s}$. The gas is chosen to be *argon* with temperature $T_0 = 0\ \text{°C}$ and density $\rho = 1.78\ \text{kg/m}^3$. Argon is chosen in place of air in our study is because a single element gas is simpler in the DSMC method. Since the Mach number is low and the Knudsen number is high, the flow field is nearly isothermal. While argon has a different heat capacity from a nitrogen - oxygen mixture due to the fact that it does not have rotation, this difference is not important in isothermal flows. Also the molecular mass and diameter of argon is similar to those of nitrogen and oxygen. So argon is a good candidate for simulating air without considering the molecule's rotation.

The flow and the system geometry are symmetric about the plane which crosses the center line of the slider along the length direction and is perpendicular to both the disk and the slider surfaces. So only half of the system is used in all simulations. In order to do this, we put a fully elastic wall at the plane of symmetry.

The number of particles needed for the half system is about 250,000 initially. Then particles will accumulate inside the control volume and get to an equilibrium stage when the flow is in its steady state. The number of cells is 10,000, 80 cells in the length direction, 25 cells in the width direction (covered half width) and 5 cells in the height direction. Since the slider has a pitch angle, some cells cross the slider surface and some other cells are simply outside the control

volume. The volume of a cell outside the control volume can not be used and is subtracted from the total cell volume. The largest cell volume is about 18% of a cubic mean-free-path of argon atoms. There is an average of 35 particles in each cell initially and every particle represents about 15 to 30 real argon atoms.

Conventional solutions (i.e. the MGL model) were obtained numerically by using the multi-grid control volume method. All the DSMC simulations were run on the IBM RS/6000 workstations. The results of the MGL model and DSMC model are compared with minimum spacings ranging from 25 nm to 2 nm. Selected 3-D pressure distributions of both simulations are shown in Figs. 3 - 5, to be discussed later.

Figure 2 shows a plot of the particle accumulation inside the control volume as a function of time for $H_{\min} = 4$ nm ($Kn = 15.63$). The points on the curve are separated by 500 time steps. There are initially 250,000 particles inside the control volume. The number increases with time and fluctuates about the steady state number of 337,000 after about 0.45 μ sec. The sampling function starts at 0.54 μ sec and last for about 50,000 time steps. Figure 2 also shows the similar curve for $H_{\min} = 15$ nm ($Kn = 4.17$). The particle accumulation starts from 250,000 and begins to fluctuate around 292,000 after about 0.38 μ sec. In this case, the flow reaches its steady state earlier than in the case with smaller minimum spacing. In addition, every particle represents more argon atoms due to the larger control volume in this case. So it accumulates fewer particles at the steady state than in the case with smaller minimum spacing to match the real number of the argon atoms in the control volume.

Figure 3(a) shows pressure plots from the DSMC solution while Fig. 3(b) shows the corresponding results from the Reynolds equation solution for the case $H_{\min} = 25$ nm ($Kn = 2.5$). The top two plots in Fig. 3(a) show the DSMC pressure profile viewed from the side and front.

The lower left plot in Fig. 3(a) shows the contours of the pressure profile. We present similar plots in Figs. 4 - 5 in which H_{\min} are 5 nm and 2 nm, respectively.

Comparing Fig. 3(a) and Fig. 3(b), we notice that the two results agree well with each other. We then lower the flying height of the slider (without changing anything else) from 25 nm to 5 nm and 2 nm. It turns out that very small relative differences are detected between the DSMC and Reynolds (MGL) solution. When the minimum spacing becomes smaller, it can be observed from these pressure profiles that the peak position moves toward the trailing edge of the slider and the peak value increases. The pressure gradient near the trailing edge is also higher.

In Table 1, we list the bearing force for different Knudsen numbers Kn and bearing numbers Λ (defined as $6\mu UL/(p_0 H_{\min}^2)$ and μ is the viscosity of the gas). The bearing force is defined as:

$$W = \frac{1}{g} \int_A (p - p_0) dA \quad (2)$$

where g is the gravitational acceleration. From the relative difference column, we can see that the maximum relative difference detected in the load is 3.76%. A graph of bearing force as a function of Knudsen number is plotted in Fig. 6. It shows that the MGL results are always higher than the DSMC results. In other words, DSMC will predict lower flying height than the MGL model if the loading force is the same. The flying height difference would be about 0.5 nm when the minimum spacing ranges from 10 nm to 5 nm according to the data showed in Table 1.

Figure 7 plots the bearing force relative difference between the DSMC and the MGL model as a function of Knudsen number. The relative difference increases with the Knudsen number until Kn reaches about 12.5 and then it drops quickly to 0.53 % when Kn is about 31.25. The reason for the relative difference drop is that the influence of the Knudsen number on the

bearing force reduces as the bearing number gets larger. Consider the steady 1-D Reynolds equation with the F-K slip correction⁷ for constant boundary temperature:

$$\frac{d}{dX} \left\{ \tilde{Q}_p(Kn) P H^3 \frac{dP}{dX} - \Lambda P H \right\} = 0 \quad (3)$$

\downarrow
 Poiseuille flow term

\downarrow
 Couette flow term

where $X = x / L$

$$P = p / p_0$$

$$H = h / H_{\min}$$

$$\tilde{Q}_p(Kn) = 1 + 6A Kn + \frac{12}{\pi} Kn \log(1+B Kn), \text{ with } A = 1.318889, B = 0.387361, \text{ given by}$$

Robert¹⁴ for $\alpha = 1$. When h_0 decreases, Kn increases and so \tilde{Q}_p will also increase. However, the Poiseuille flow term decreases as $H^2 \log H$ while the Couette flow term increases as H^{-1} when H approaches zero. So the Knudsen number loses its influence as the Couette flow term becomes dominant. The flow becomes independent of the Knudsen number.

Finally, we reduced the minimum spacing to zero so that the slider is actually contacting the disk at the trailing edge and the contact region is a straight line in the width direction. In this case, the particle reservoir at the trailing edge vanishes and no particle will come in or go out of the control volume through the slider's trailing edge. It should be noted that the Reynolds equation predicts unbounded pressure at zero spacing, and therefore cannot be used for contact. The pressure profile from DSMC is presented in Fig. 8. Figure 8(a) shows the contact pressure profile viewed from the side. This simulation indicates that the DSMC method can solve for cases asperity contacts which often occurs in the new slider-disk interfaces. It shows that the peak pressure is located at about 95% of the total slider length from the leading edge and is about

14.78 times the atmospheric pressure. Figure 8(b) gives a better look at the contact region. It shows that near the contact region, the pressure drops sharply from the peak value to about absolute zero. This is because in the neighborhood of the contact line, the effective cell volume is so small that there are not enough particles to provide any bearing pressure. This is a qualitatively reasonable representation of the real physical situation. Further contact simulation is already in progress.

IV. Conclusion

The slider bearing problem for very low spacing is simulated by the Direct Simulation Monte Carlo method and the results are presented in this report. The slider is a three-dimensional flat plate flying over a flat rotating disk. Results for different flying heights were obtained and compared to the numerical simulation results of the Reynolds lubrication equation with the Fukui-Kaneko slip correction. The results show that the MGL model predicts higher bearing force (or up to 0.5 nm lower flying height) than the DSMC model. Overall, the two solutions agree well with each other, and surprisingly, the agreement is better as the spacing decreases beyond about 5 nm. The largest relative difference for the bearing force is 3.76% when the Knudsen number is 12.5 and the bearing number is 4,928. The study also shows that the reason the two solutions merge at very large bearing number and the continuum model works well again, is that the effect of the Knudsen number becomes negligible.

The contact pressure profile calculated by DSMC shows that there exists a sub-ambient pressure region in front of the contact point and the pressure reduces to zero at the contact point. This example shows that the DSMC method is capable of air bearing simulation when there are points of contact. This is in contrast to the Reynolds equation, which predicts unbounded pressure at contact points.

Although the MGL model works very well for the sliders with simple 3-D geometry, it is still not clear what will happen when the slider has a more complicated geometry so that some local Knudsen number is high but the global bearing number is not so large. Will the MGL model still be capable of giving good results? In addition, when the minimum spacing approaches zero, the conventional method will predict infinitely large pressure while the DSMC

solution is still capable of dealing with quasi-contact and contact condition. Our next investigation will be to simulate a three dimensional flat slider with a spherical asperity underneath by using the Direct Simulation Monte Carlo method to determine the pressure as the spacing at the asperity approaches zero. In this way we expect to learn how to correctly modify the MGL model in situations where surface roughness leads to isolated contacts.

Acknowledgments

This project was sponsored by the Computer Mechanics Laboratory at UC Berkeley and IBM through a Predoctoral Fellowship (WH) and a Shared University Grant. The work is also supported in part by a grant to ALG from the National Science Foundation. We are grateful to S. Bolasna for his interest and discussions.

References

¹MGL stands for the Molecular Gas Film Lubrication

²BGK model is after Bhatnager, Gross, and Krook (1954).

³F. J. Alexander, A. L. Garcia, and B. J. Alder, “Direct Simulation Monte Carlo for Thin-Film Bearings,” *Phys. Fluids A* 6, 3854 (1994).

⁴P. L. Bhatnagar, E. P. Gross and M. Krook, “A Model for Collision Processes in Gases. I. Small Amplitude Processes in Charged and Neutral One-Component Systems,” *Phys. Rev.*, 94, 511 (1954).

⁵G. A. Bird, *Molecular Gas Dynamics and the Direct Simulation of Gas Flows* (Clarendon Press, Oxford, 1994).

⁶A. Burgdorfer, “The Influence of the Molecular Mean Free Path on the performance of Hydrodynamic Gas Lubricated Bearings,” *ASME J. Basic Eng.*, 81, 94 (1959).

⁷S. Fukui and R. Kaneko, “Analysis of Ultra-Thin Gas Film Lubrication Based on Linearized Boltzmann Equation: First Report--Derivation of a Generalized Lubrication Equation Including Thermal Creep Flow,” *ASME J. of Tribology*, 110, 253 (1988).

⁸S. Fukui and R. Kaneko, “A Database for Interpolation of Poiseuille Flow Rates for High Knudsen Number Lubrication Problems,” *ASME J. of Tribology*, 112, 78 (1990).

⁹S. Fukui, R. Matsuda and R. Kaneko, “On the Physical Meanings of Λ/\tilde{Q}_{po} and σ/\tilde{Q}_{po} in Molecular Gas Film Lubrication Problems,” *ASME/STLE Tribology Conference*, Orlando, FL (1995).

¹⁰Y. T. Hsia and G. A. Domoto, “An Experimental Investigation of Molecular Rarefaction Effects in Gas Lubrication Bearings at Ultra-Low Clearances” ASME, J. of Lubrication Technology, 105, 120 (1983).

¹¹F. C. Hurlbut, 1996, “Rarefied-Gas Dynamics, ” Encyclopedia of Applied Physics, 16, 97 (1996).

¹²A. L. Garcia, *Numerical Methods for Physics* (Prentice-Hall, Englewood Cliffs, New Jersey, 1994), Chap. 10.

¹³R. Matsuda and S. Fukui, “Ultra-Thin Gas Squeeze Film Characteristics for Finite Squeeze Numbers, ” ASME/STLE Tribology Conference, Orlando, FL (1995).

¹⁴M. Robert, “New Implamentation of Boltzmann Correction to Lubrication Theory, ” IBM Research Report (1993)

¹⁵Y. Takeuchi, K. Tanaka, S. Odaka and F. Muranushi, “Examination of Flying Height of Magnetic Head Slider between Simulations and Measurements Taking into Account Zero-Spacing Error, ” Trans. JSME (Ser. C), 60, 2547 (1994).

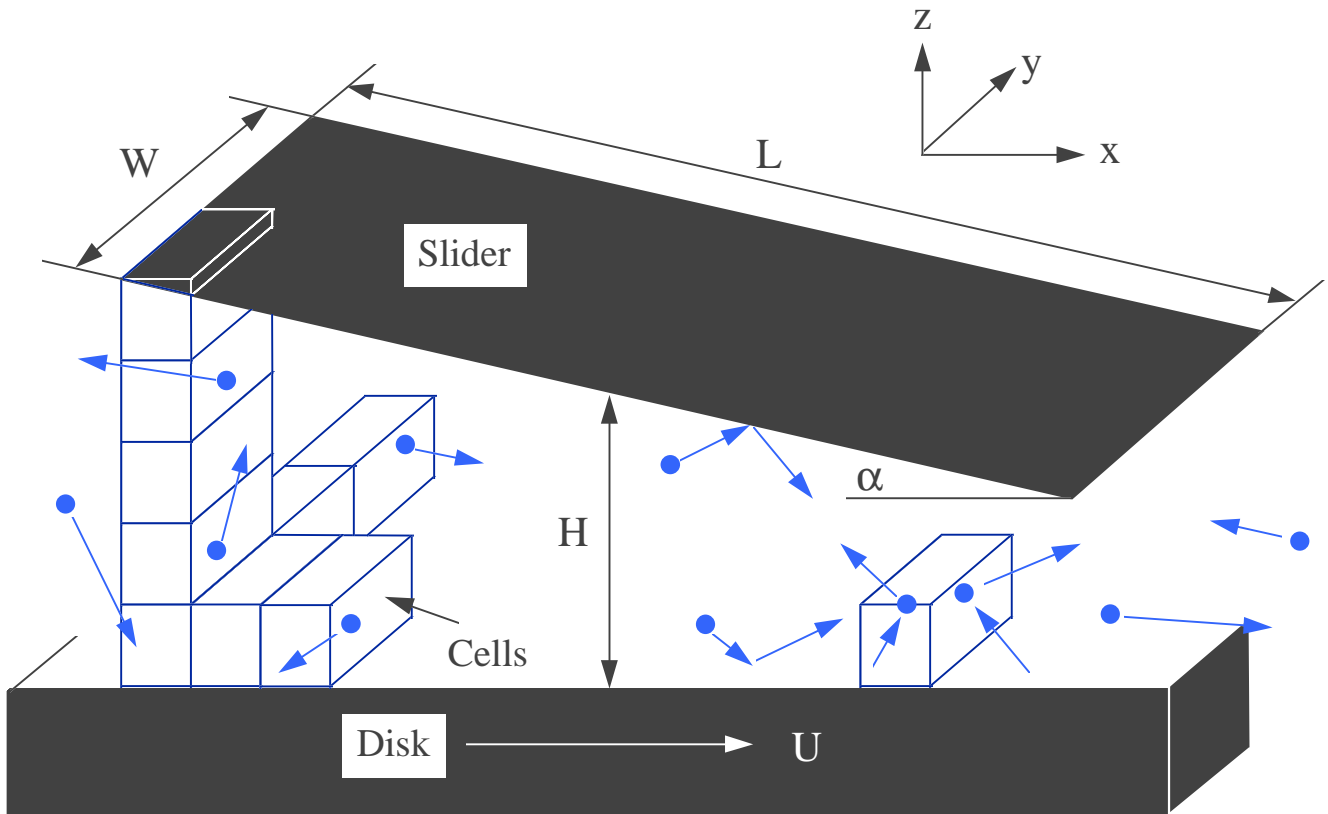


Fig. 1. DSMC System Configuration

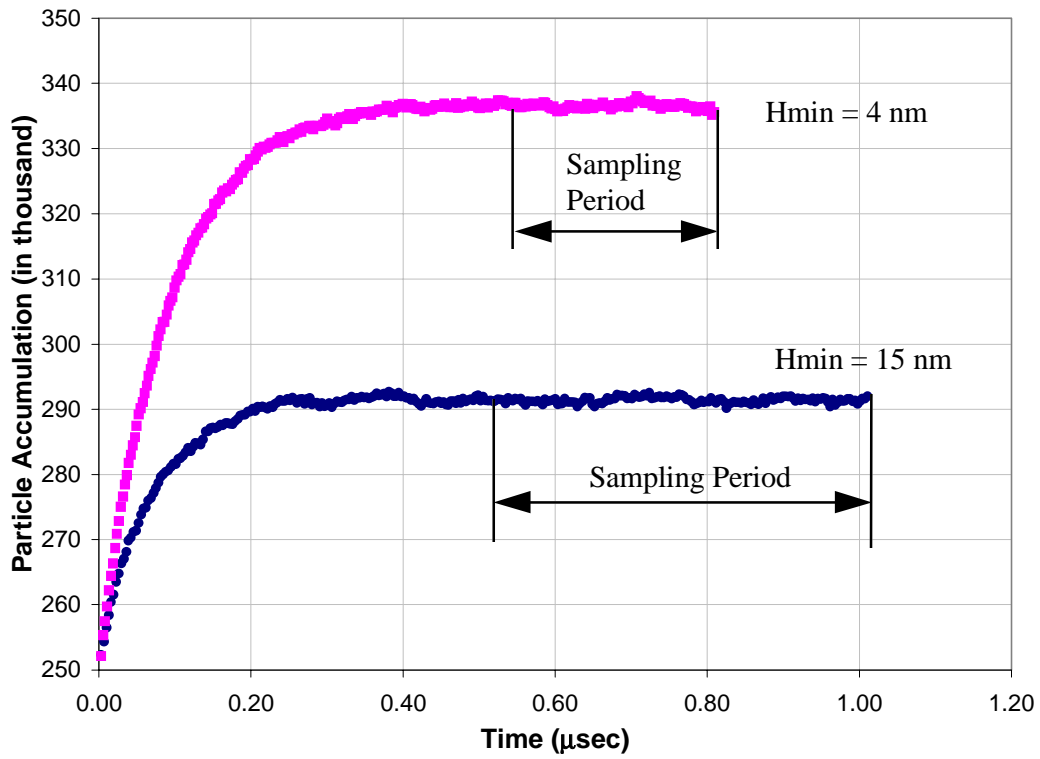
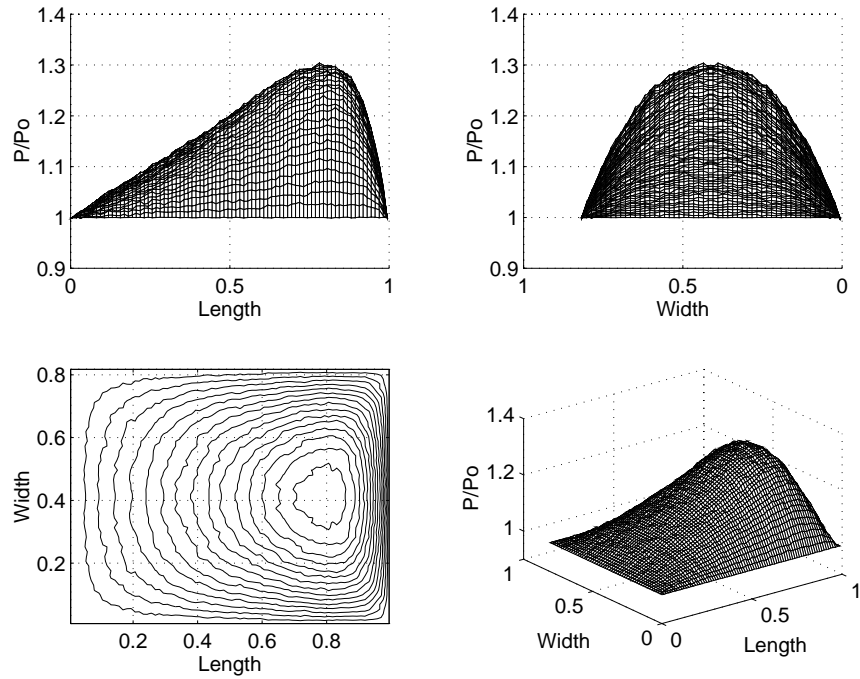
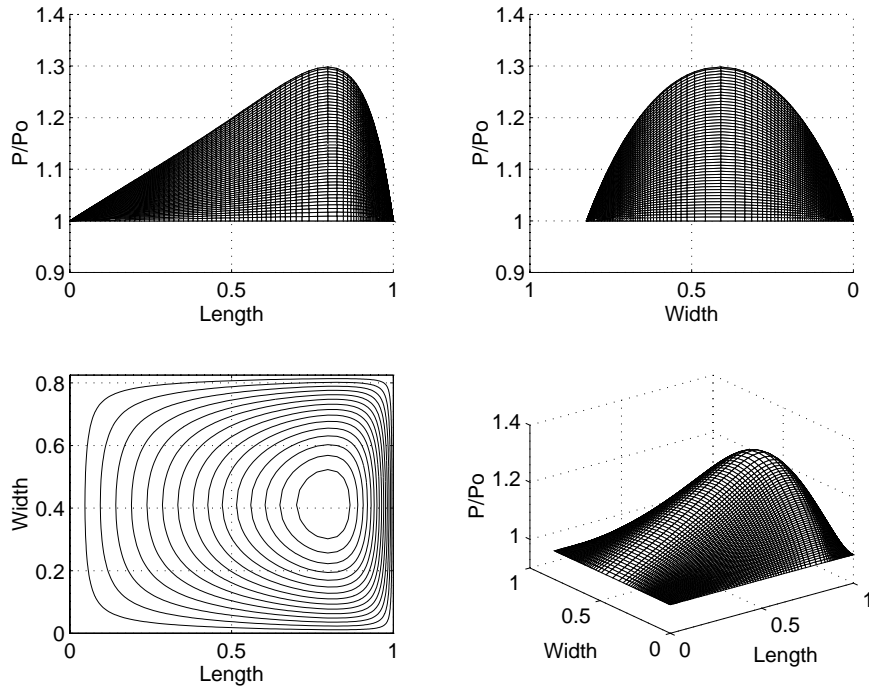


Fig. 2 Particle Accumulation Curve



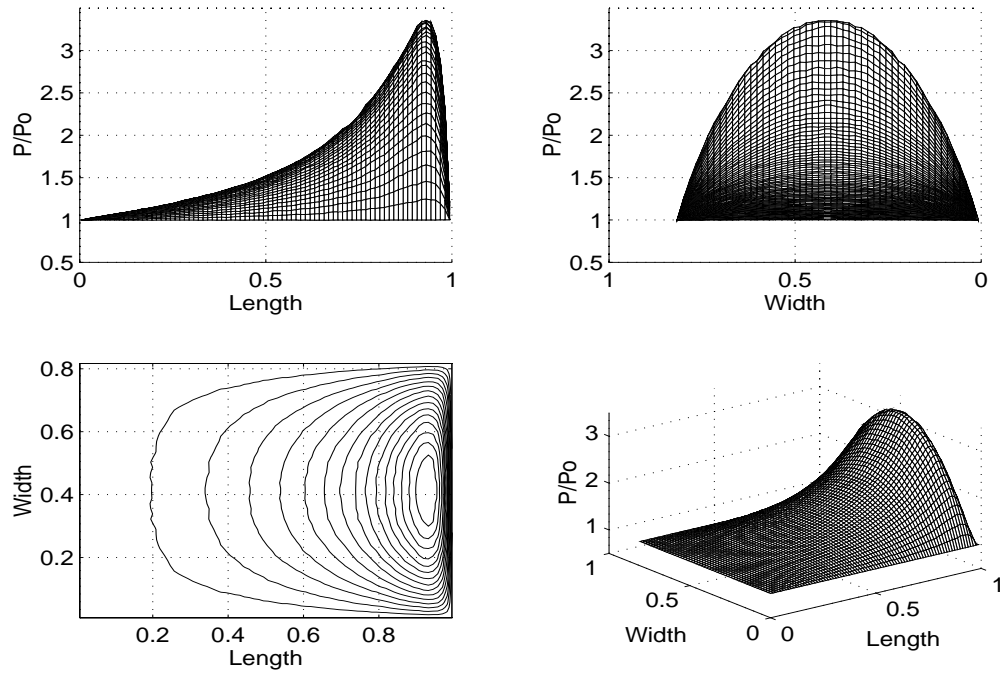
(a)



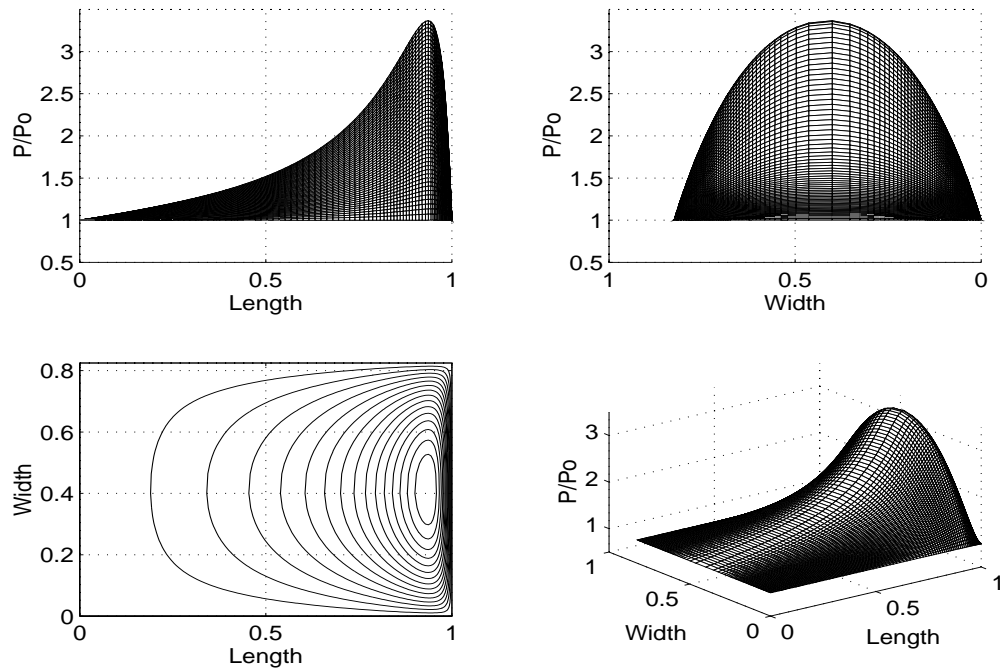
(b)

Fig. 3. 3-D Pressure Profile for $Kn = 2.5$ ($H_{\min} = 25$ nm)

(a) DSMC Result (b) MGL Result



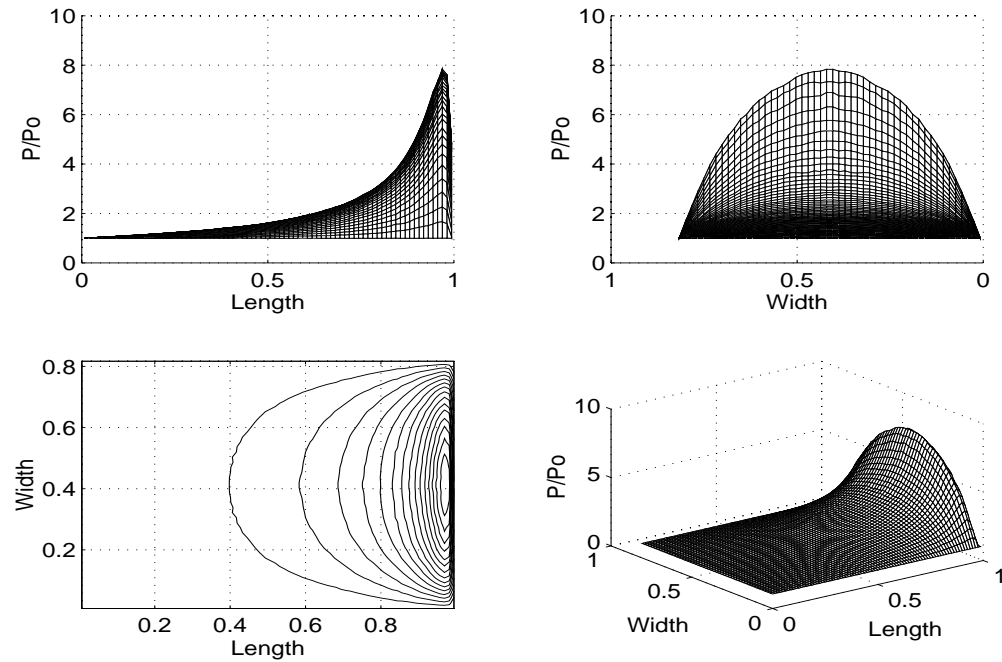
(a)



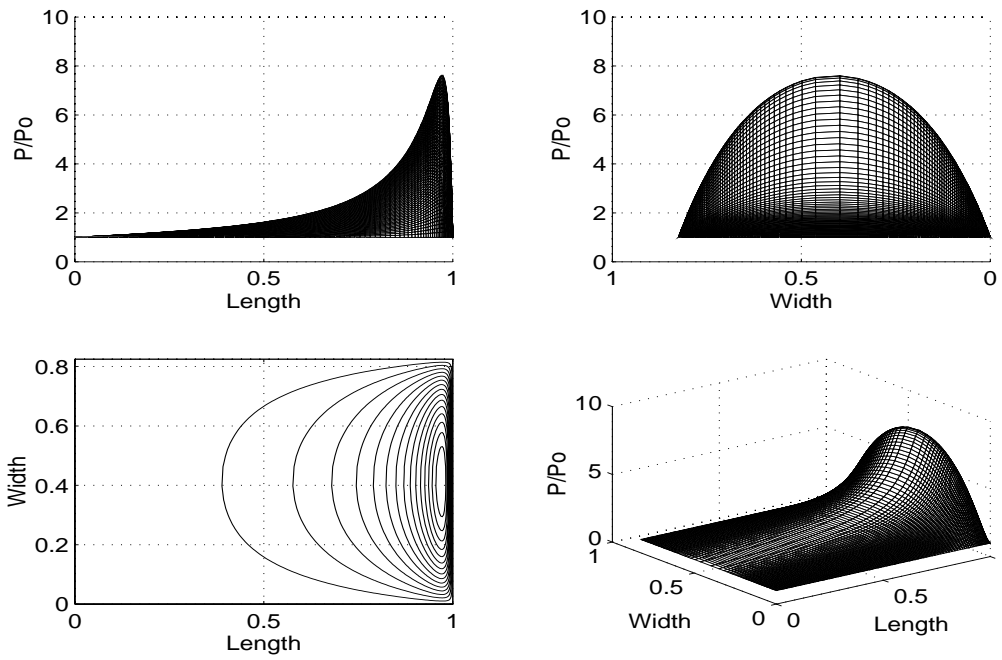
(b)

Fig. 4. 3-D Pressure Profile for $Kn = 12.5$ ($H_{min} = 5$ nm)

(a) DSMC Result (b) MGL Result



(a)



(b)

Fig. 5. 3-D Pressure Profile for $Kn = 31.25$ ($H_{\min} = 2$ nm)

(a) DSMC Result (b) MGL Result

H_{min} (nm)	K_n	Λ	Bearing Force (x 10⁻² mg)		Rel. Difference
			DSMC	MGL	
25	2.5	197	1.571	1.594	1.46 %
20	3.13	308	2.019	2.070	2.52 %
15	4.17	548	2.753	2.823	2.54 %
10	6.25	1,232	4.028	4.167	3.42 %
5	12.5	4,928	6.950	7.212	3.76 %
4	15.63	7,700	8.180	8.373	2.36 %
3	20.83	13,689	9.835	9.979	1.46 %
2	31.25	30,800	12.355	12.420	0.53 %

Table 1. Bearing Force

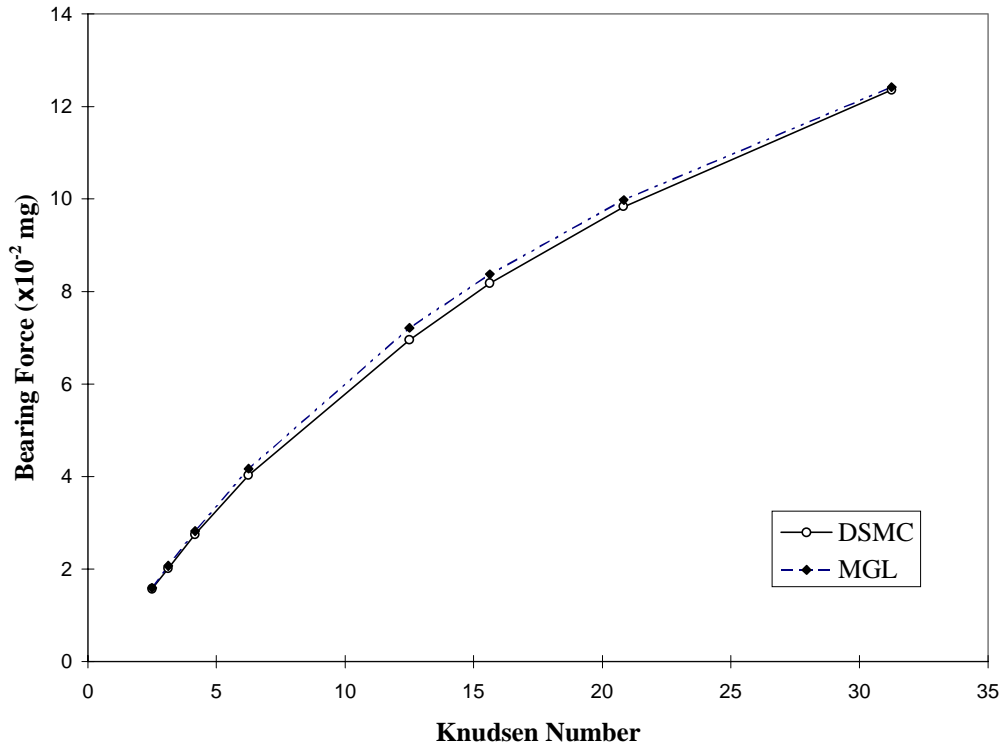


Fig. 6. Bearing Force Vs. Knudsen Number

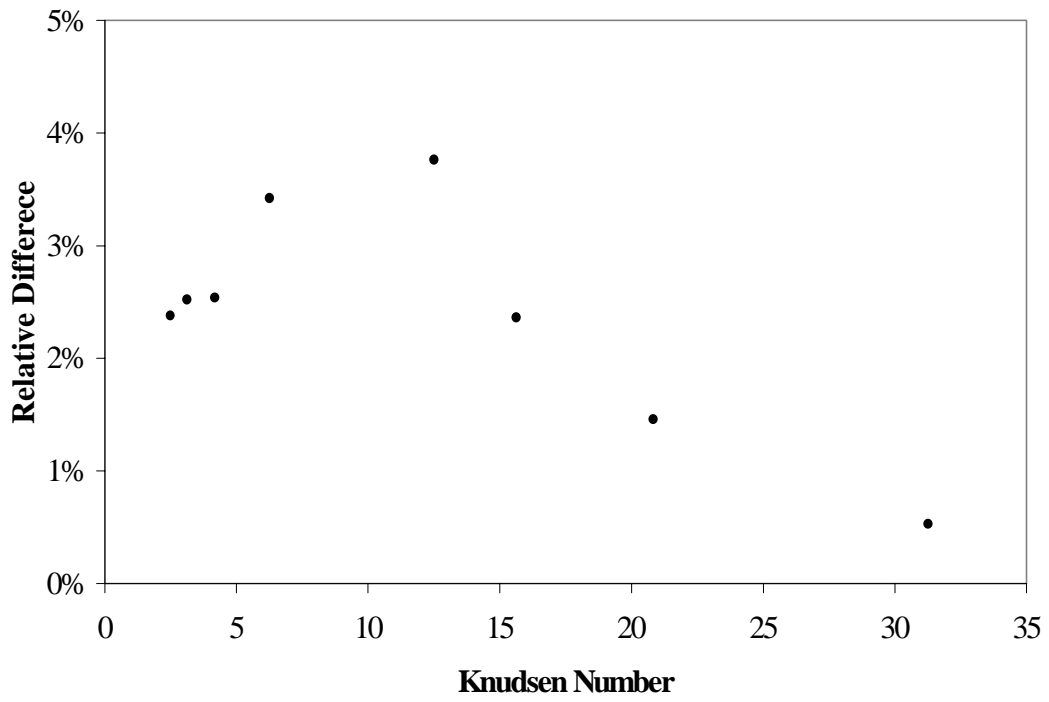


Fig. 7. Relative Bearing Force Difference between DSMC and MGL model

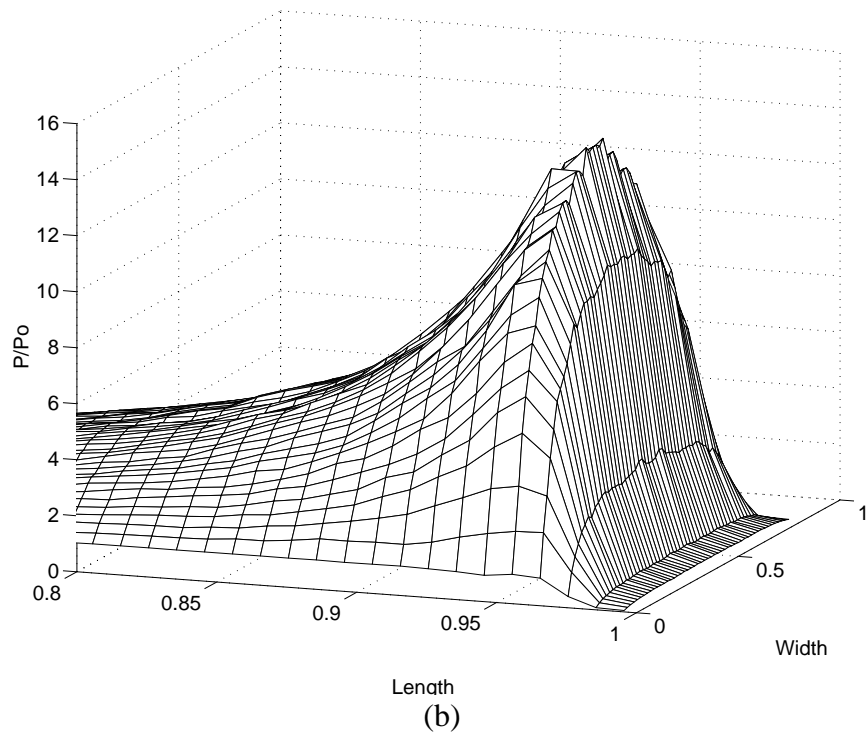
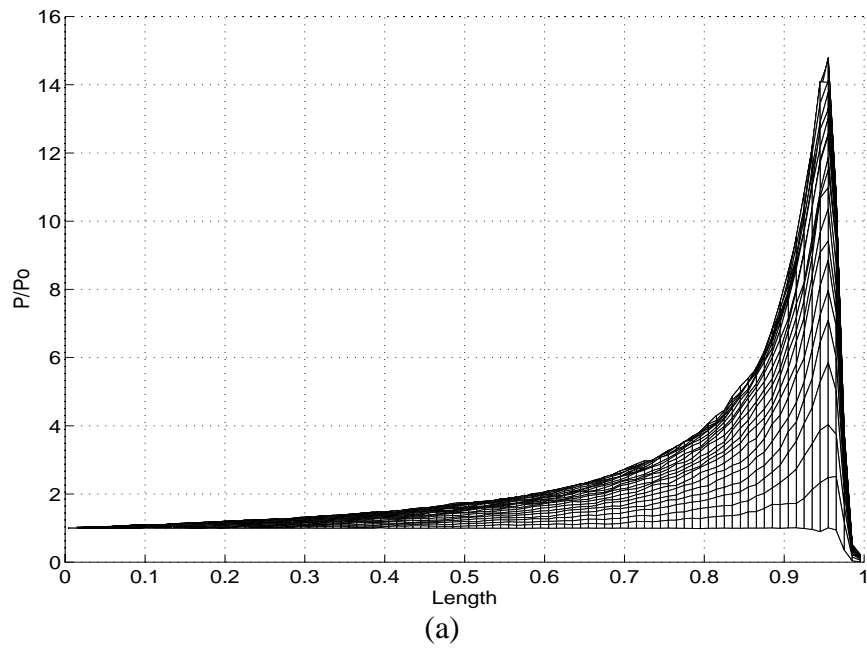


Fig. 8. Pressure Profile for $Kn = \infty$ ($H_{min} = \text{Zero nm}$)

(a) Side view (b) 3-D view